



The Society shall not be responsible for statements or opinions advanced in papers or in discussion at meetings of the Society or of its Divisions or Sections, or printed in its publications. Discussion is printed only if the paper is published in an ASME Journal. Released for general publication upon presentation. Full credit should be given to ASME, the Technical Division, and the author(s). Papers are available from ASME for nine months after the meeting.  
Printed in USA.

Copyright © 1985 by ASME

## Directionally Solidified DS CM 247 LC—Optimized Mechanical Properties Resulting From Extensive $\gamma'$ Solutioning

G. L. ERICKSON, K. HARRIS and R. E. SCHWER

Cannon-Muskegon Corporation

P.O. Box 506

Muskegon, Michigan 49443

USA

### ABSTRACT

Complete coarse  $\gamma'$  and greater than 90% eutectic  $\gamma$  -  $\gamma'$  solutioning, without incipient melting, is demonstrated for the DS CM 247 LC superalloy. This unusual capability for this advanced Ni-base turbine blade and vane material results in considerable mechanical properties enhancement, with the DS alloy capability being near to current single crystal superalloys in the 345-207 MPa, 871°C-982°C (50-30 ksi, 1600°F-1800°F) operating condition. Microstructural features are detailed correlating strength and alloy stability.

### NOMENCLATURE

|             |                                |
|-------------|--------------------------------|
| AC          | - Air Cool                     |
| DS          | - Directional Solidification   |
| GFQ         | - Gas Fan Quench               |
| HCF         | - High Cycle Fatigue           |
| LCF         | - Low Cycle Fatigue            |
| MC-1        | - Ti rich carbide              |
| MC-2        | - Ta rich carbide              |
| MC-3        | - Hf rich carbide              |
| $M_6C$      | - W, Mo rich secondary carbide |
| $M_{23}C_6$ | - Cr rich secondary carbide    |
| RT          | - Room Temperature             |
| $V_f$       | - Volume Fraction              |
| VIM         | - Vacuum Induction Melting     |
| $\gamma$    | - Gamma                        |
| $\gamma'$   | - Gamma Prime                  |
| $\sigma$    | - Sigma Phase                  |
| $\mu$       | - Mu Phase                     |
| $\alpha$ W  | - Alpha-Tungsten Phase         |

### INTRODUCTION

Ni-based superalloys are referred to as "superalloys" due to their ability to exhibit outstanding strength at temperatures as great as 85% of their melting points ( $0.85 T_m$ ). Such alloys consist of an austenitic FCC matrix ( $\gamma$ ), dispersed inter-

metallic FCC gamma prime ( $\gamma'$ ) precipitate that is coherent with the matrix, plus carbides, borides and other phases which are distributed throughout the matrix and along the grain boundaries. Property attainment with superalloys is principally a function of a) the amount and morphology of the  $\gamma'$ , b) grain size and shape, and c) carbide distribution.

Superalloys have evolved over the last 50 years with most development work stimulated by demands of the advancing gas turbine engine technology. Cast, equiaxed superalloy development was fast-moving and highly rewarding up through the 1960's, with such activity resulting from the introduction of commercial vacuum induction melting and vacuum investment casting in the early 1950's (Fig. 1, Ref. 1). However, once the developing alloys became "super-saturated" in terms of  $\gamma'$  volume fraction, more attention was placed on casting process development, e.g., directional solidification.

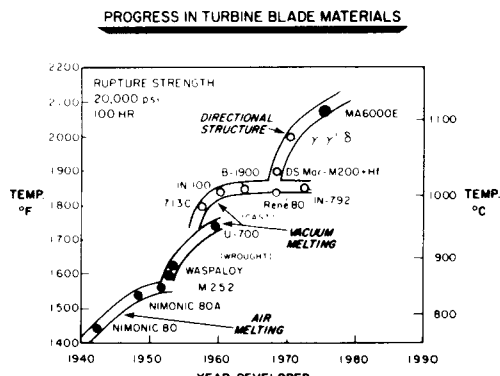


Figure 1. Progress in the Temperature Capability of Superalloys in the Last 40 Years (Ref. 1).

Substantiating these efforts, directionally solidified (DS) superalloy turbine airfoils began appearing in military application during the mid-1960's. Commercial engine application of such followed in the late 1960's and early 1970's, with turbine engine builders utilizing more than 1 million DS airfoils to date. Significant mechanical property advantages are attained with directionally solidified superalloy turbine airfoils, relative to those conventionally cast; specifically, greater thermal fatigue (8X), rupture life (2X), and rupture ductility (4X) (Ref. 2).

Although the strength advantages attained with DS processing are well established and many DS production castings have been produced during the last 10-15 years, relatively few alloys realize production application. The fact that relatively few, really good DS superalloys exist, again, is a function of industry R&D emphasis being placed more on process rather than alloy development during this period. Of course, some of the well established equiaxed superalloys, modified slightly (Hf introduction) to facilitate improved DS castability, are utilized in DS application. However, some alloys exhibit grain boundary cracking problems during directional solidification, or metal/core reaction tendency with resultant HfO inclusion problems (due to relatively high Hf level), when cast into today's complex-cored, thin wall airfoils.

In an attempt to develop an alloy which would overcome these problems, Cannon-Muskegon derived the DS CM 247 LC alloy from the base Mar M 247 composition. The primary alloying modifications are the reduction of C by approximately one-half to improve carbide microstructure, stability, and alloy ductility, plus the tailoring of the Zr and Ti contents to improve DS grain boundary cracking resistance without sacrificing strength (Table I). Additionally, the alloy's W and Mo levels are slightly reduced to compensate for the lower C and Ti concentration, thereby minimizing the formation of deleterious secondary  $M_6C$  platelets,  $\mu$  phase and/or alpha W platelets or needles due to the degeneration of primary carbides with high temperature exposure. This degeneration or breakdown of the low parameter MC-1 (Ti rich) and MC-2 (Ta rich) carbides to form the higher parameter MC-3's (Hf rich) results in the release of Ta and some Ti to the solid solution, thereby changing the solubility of the W and Mo in the basic gamma solid solution; the result of such being the possible formation of  $\mu$  phase, alpha W and/or  $M_6C$ , depending on temperature (Ref. 3). More detail regarding the early (1978) DS CM 247 LC development activity is presented in Reference 4. The alloy has also been evaluated in integral turbine wheel application due to its desirable carbide morphology characteristics (LCF considerations), excellent ductility and creep strength, with such being reviewed in Reference 5 and 6. Additionally, further DS production data and review is presented in Reference 7.

In terms of the alloy's DS process castability, the evaluation test developed by the General Electric Company during the G.E. René 150 development (Ref. 8) shows DS CM 247 LC to be superior in grain boundary cracking resistance to Mar M 247. The test essentially casts a thin-walled DS tube about an alumina core with the resultant solidification

Table I.

**MAR M 247/CM 247 LC  
NOMINAL COMPOSITIONS  
(Wt. %)**

|    |           |    |             |
|----|-----------|----|-------------|
| C  | 0.15/0.07 | Al | 5.5/5.6     |
| Cr | 8.4/8.1   | Ti | 1.0/0.7     |
| Co | 10.0/9.2  | Hf | 1.5/1.4     |
| W  | 10.0/9.5  | B  | 0.015/0.015 |
| Mo | 0.7/0.5   | Zr | 0.05/0.015  |
| Ta | 3.0/3.2   | Ni | BAL/BAL     |

strain being approximately 2%. Grain-boundary cracking occurs in crack-susceptible alloys, with ratings ranging from A (no cracking) to F (gross grain-boundary cracking). Such a test, undertaken with DS CM 247 LC and Mar M 247, results in no apparent cracks in the DS CM 247 LC tube (A-rating) and considerable grain-boundary cracking in the Mar M 247 tube (E-rating) (Ref. 7). Recent work with 1.0% Hf containing DS CM 247 LC (the typical Hf level encountered in cored airfoils cast with the 1.4% Hf containing CM 247 LC alloy) shows a similar A-rating with no cracking.

So, with the DS CM 247 LC alloy possessing excellent DS castability and "baseline" mechanical property data existing for the alloy solutioned at the 1221°C/2 hr. condition, the thrust of the current program is toward maximizing the alloy's mechanical property response, relative to the "baseline", through optimized solutioning and aging procedures. The program is still in process. This writing represents an interim report.

**EXPERIMENTAL PROCEDURE**

DS CM 247 LC alloy is produced utilizing Cannon-Muskegon vacuum induction melting technology (Ref. 9). Bar stock from two different CM, 3629 kg. (8000 lb.) master heats, i.e., V6550 and V6692, supplied to two major precision investment casters, as well as a turbine engine producer captive foundry for test specimen manufacture, is examined. Both DS bar and slab product (respective sizes as outlined in Table III) are utilized in chemistry overchecks and the heat treat investigation.

Solution heat treatment is performed in a Lindberg tube furnace (Model 59545, accurate to  $\pm 2^\circ\text{C}$ ) according to the conditions presented in Table II. All specimens are air-cooled. Standard metallographic technique is applied in preparing the test specimens for optical microstructural review with a Nikon Epiphot instrument.

Table II.

**DS CM 247 LC SOLUTIONING CONDITION MATRIX**

**Single-Step Solution ( $^\circ\text{C}/2$  Hrs./A.C.)**

- 1204°C
- 1216°C
- 1221°C
- 1227°C
- 1232°C

**Two-Step Solution ( $^\circ\text{C}/2$  Hrs. +  $^\circ\text{C}/2$  Hrs./A.C.)**

- 1204°C + } 1243°C; 1249°C; 1254°C; or
- 1216°C + } 1260°C
- 1221°C + }
- 1227°C + }
- 1232°C + } 1243°C; 1249°C; 1254°C; or  
1260°C; 1266°C; or 1271°C

Single-step solutioning, undertaken with 1.6 cm square specimens, is used to evaluate the degree of microstructural homogenization and solutioning attainable with the alloy after a 2 hour soak period. Two-step solutioning is investigated using DS slab specimens, 6.4 cm x 1.6 cm x 1.6 cm, each initially "pre-homogenized", sectioned into fourths (apart from the 1232°C "pre-homogenized" specimen, which is sliced into six pieces), and then further treated according to Table II conditions.

Microstructural characterization of the heat treated specimens is undertaken and an optimum solutioning procedure selected for the mechanical test, alloy stability, DS casting process and aging treatment investigations.

Both slab and bar specimens are heat treated according to the optimized conditions (1232°C/2 hrs. + 1260°C/2 hrs./AC + pseudo coat and aging) and subjected to RT - 871°C longitudinal and RT - 982°C transverse tensile, plus 760°C-1093°C longitudinal and transverse stress- and creep-rupture testing. Failed stress- and creep-rupture samples are reviewed for signs of instability, along with specimens which are soaked at 982°C and 1038°C for 500 and 1000 hours each, respectively. Additionally, identically solutioned slabs are used to study the effects of various aging treatments, e.g., 1079°C/4 hrs., 982°C/5 hrs., 1050°C/16 hrs., 871°C/20 hrs., and 899°C/16 hrs.

## RESULTS AND DISCUSSION

### Chemistry Overchecks

The DS CM 247 LC aim chemistry is balanced to provide excellent DS process castability and strength potential. Owing to this chemistry balancing, the alloy also exhibits a reasonable heat treatment "window" (difference between the alloy's  $\gamma'$  solvus and incipient melting temperatures) and relatively high incipient melting point, which makes the alloy amenable to high temperature heat treatment, such allowing for extensive  $\gamma'$  and eutectic  $\gamma - \gamma'$  solutioning.

Features such as DS grain boundary cracking resistance and heat treatment "window" are extremely chemistry sensitive, with the severity dependent upon the alloy. Maintaining proper chemistry balance through precision investment casting application is crucial. Table III shows some of the elements which must be tightly controlled in the CM 247 LC alloy to maintain its performance capability. Note that pick-up of Si and Zr occurs as a function of molten metal contact time with the investment casters melt crucible and/or shell system. Additionally, Hf loss occurs as a relation of the same. DS test specimen gas levels are quite satisfactory, indicating excellent mold pre-heat/out-gassing (inherent with DS) and vacuum furnace leak-tightness. Al + Ti levels are maintained with the exception of one set of specimens.

Severe Si and Zr pick-up could lead to increased DS grain-boundary cracking tendency during casting production, however, the level of pick-up required for such a consequence is not investigated herein. Inclusions associated with high gas level are found to affect DS grain yield, therefore making tight

Table III.

DS CM 247 LC SELECTED CHEMISTRY DETAIL  
MASTER HEAT VS. INVESTMENT CAST SPECIMENS

| Element | Master Heat<br>V6692 | TRW DS Slab *<br>Bottom | TRW DS Slab *<br>Top | Rolls Royce DS Slab **<br>Bottom | Rolls Royce DS Slab **<br>Top |
|---------|----------------------|-------------------------|----------------------|----------------------------------|-------------------------------|
| C       | .070                 | .070                    | .067                 | .070                             | .070                          |
| Si      | .003                 | .005                    | .014                 | .009                             | .010                          |
| Zr      | .018                 | .022                    | .023                 | .021                             | .018                          |
| Al      | 5.65                 | 5.12                    | 5.70                 | 5.68                             | 5.68                          |
| Ti      | .69                  | .68                     | .68                  | .70                              | .68                           |
| Hf      | 1.4                  | 1.39                    | 1.36                 | 1.49                             | 1.22                          |
| [N] ppm | 3                    | 2                       | 2                    | 3                                | 2                             |
| [O] ppm | 3                    | 2                       | 2                    | 3                                | 3                             |
| S ppm   | 5                    | 6                       | 6                    | 6                                | 7                             |

| Element | Master Heat<br>V6550 | AETC DS Slab *<br>Bottom | AETC DS Slab *<br>Top | TRW DS Bar **<br>Bottom | TRW DS Bar **<br>Top |
|---------|----------------------|--------------------------|-----------------------|-------------------------|----------------------|
| C       | .071                 | .075                     | .076                  | .072                    | .070                 |
| Si      | .007                 | .004                     | .006                  | .008                    | .009                 |
| Zr      | .020                 | .024                     | .023                  | .025                    | .023                 |
| Al      | 5.55                 | 5.48                     | 5.50                  | 5.58                    | 5.60                 |
| Ti      | .70                  | .63                      | .63                   | .68                     | .66                  |
| Hf      | 1.4                  | 1.26                     | 1.06                  | 1.41                    | 1.23                 |
| [N] ppm | 2                    | 2                        | 3                     | 2                       | 2                    |
| [O] ppm | 1                    | 1                        | 1                     | 2                       | 2                    |
| S ppm   | 6                    | 8                        | 8                     | 6                       | 7                    |

Analyses in wt. % unless otherwise indicated.

\* 1.6 cm x 1.4 cm x 11.4 cm 3.

\* b.6 cm x 1.3 cm dia. x 14.5 cm 1.

\*\* 4.1 cm x 10.2 cm x 13.7 cm 1.

control of [N] and [O] and overall alloy cleanliness extremely important. Of course, Al + Ti fade results in inclusion formation and mechanical property deterioration. Sulfur, tending to migrate to grain boundaries, can decrease hot ductility and promote cracking during component application (Ref. 10), thereby suggesting it be closely controlled as well. Minimization of shell or core system reactivity with Hf containing alloys must be achieved, otherwise hafnium oxide formation may occur at the expense of overall alloy Hf content, potentially causing variation in terms of component cleanliness, grain yield, carbide morphology and eutectic  $\gamma - \gamma'$  characteristics. Noteworthy is that the severity of Hf loss and Si plus Zr pick-up increased in the top of the specimen relative to the bottom, an effect of the longer molten alloy contact time in the mold.

### Single-Step Solutioning

Figure 2 shows a typical as-cast, DS CM 247 LC slab microstructure. Review of specimens solution heat treated from 1204°C to 1232°C reveals that coarse  $\gamma'$  solutioning initially occurs at 1216°C, with the degree of such increasing with greater

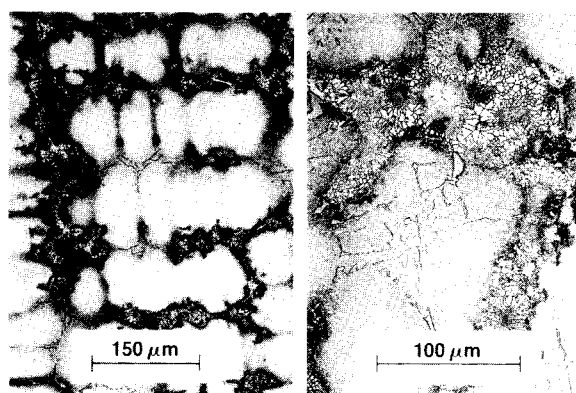


Figure 2. DS CM 247 LC as-cast microstructure.  
Section size: 1.6 cm.

temperature. Significant eutectic  $\gamma$  -  $\gamma'$  solutioning is not realized except at the 1232°C/2 hr. condition, an example of such being shown in Figure 3. Ancillary investigation shows the alloy's  $\gamma'$  solvus is approximately 1249°C and its single-step solution procedure incipient melting point is approximately 1257°C, both being determined metallographically.

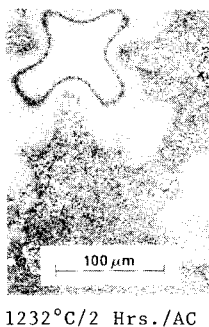


Figure 3. DS CM 247 LC single-step solutioning.

The increased solutioning achieved at the 1232°C/2 hr. soak condition, relative to lower temperature solutioned specimens, effects improved creep-rupture life due to an increased effective volume fraction of fine, reprecipitated  $\gamma'$  (given the fixed total amount of  $\gamma'$ ). This effect confirms that reported for the DS Mar M 200 Hf alloy in Reference 11 (Fig. 4).

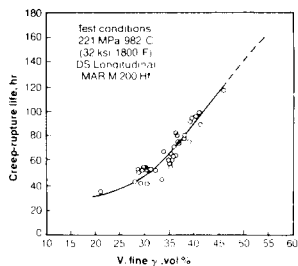


Figure 4. DS Mar M 200 Hf rupture life vs. volume fraction ( $V_f$ ) fine  $\gamma'$  at a fixed total amount of fine and coarse  $\gamma'$  (Ref. 11).

The creep-rupture benefit gained with the 1232°C/2 hr. single-step solutioned specimens is slight relative to the baseline 1221°C/2 hr. capability since the alloy's volume fraction of fine  $\gamma'$  is only marginally increased. More efficient solutioning gained with step-treatment procedure results in more significant property enhancement, as follows.

#### Two-Step Solutioning

More efficient solutioning of the DS CM 247 LC alloy is realized by step-solutioning, thereby effecting homogenization of the cast, segregated structure prior to a final, high-temperature treatment. The homogenization effectively raises the alloy's incipient melting point, consequently allow-

ing much more flexibility in the choice of a final treatment temperature; this being quite important when attempting to maximize eutectic  $\gamma$  -  $\gamma'$  solutioning.

Owing to the alloy's relatively high incipient melting point (~ 1270°C with pre-homogenization and ~ 1257°C without), high temperature treatment can be undertaken, with significant homogenization/solutioning of the segregated structure occurring in a reasonable time without incipient melting. Some  $\gamma'$  super-saturated DS alloys possess lower incipient melting and  $\gamma'$  solvus points, e.g., Mar M 247, making extensive  $\gamma'$  solutioning (apart from the dendrite cores) difficult within a reasonable period of time, with incipient melting potentially occurring in the segregated interdendritic regions. With DS CM 247 LC, however, complete coarse  $\gamma'$ , along with considerable eutectic  $\gamma$  -  $\gamma'$  solutioning, occurs without incipient melting. This extensive eutectic  $\gamma$  -  $\gamma'$  solutioning capability (as shown in Fig. 5 for the specimens treated at 1232°C/2 hrs. + 1260°C/2 hrs./AC) is felt to be primarily related to the alloy's chemistry balance -- minimized supersaturation -- and resulting "willingness" for the gamma solid solution to accept Ta, Ti and Hf (some of which may participate in secondary carbide formation--MC-3). Comparable "willingness" for  $\gamma'$  solutioning is not exhibited by other production DS alloys such as Mar M 247; this being shown in Figure 6 for a 1221°C/2 hrs./GPO solutioned blade section, where relatively minor  $\gamma'$  solutioning is apparent. It is unlikely that even long duration solutioning of the standard Mar M 247 alloy near its reported incipient melting point of 1240°C will result in any eutectic  $\gamma$  -  $\gamma'$  solutioning, with coarse  $\gamma'$  movement being incomplete (Ref. 12).

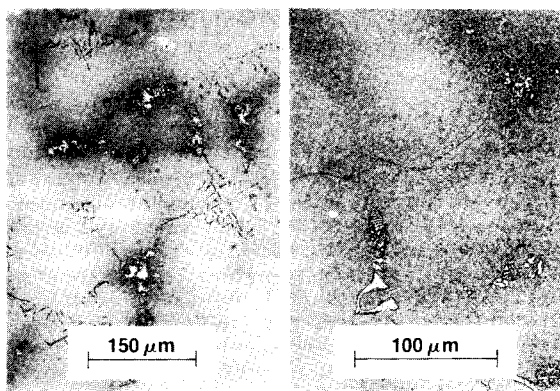


Figure 5. DS CM 247 LC solution treated at 1232°C/2 Hrs. + 1260°C/2 Hrs./AC.

Complete coarse  $\gamma'$  solutioning occurs in all DS CM 247 LC specimens pre-homogenized between 1216°C and 1232°C for 2 hours, having the common final solution step of 1260°C/2 hrs./AC. Eutectic  $\gamma$  -  $\gamma'$  solutioning is found to be maximized by increasing the homogenization-step temperature; plus it appears that microstructural homogenization, initially effected with the 1216°C, 1221°C and

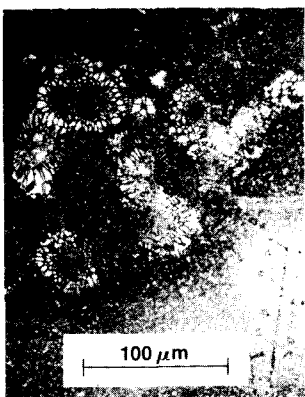


Figure 6. DS Mar M 247 solution treated at 1221°C/2 Hrs./GFQ.  
Section size: 0.3 cm.

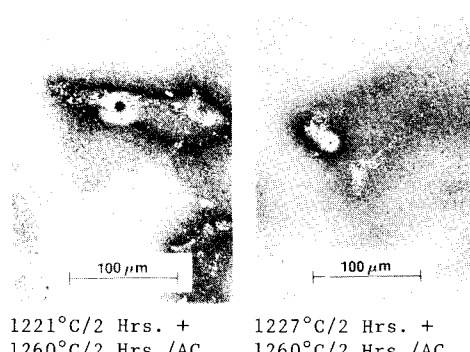


Figure 7. DS CM 247 LC two-step solutioning showing incipient melting due to incomplete homogenization.

1227°C respective pre-treatment, is insufficient due to the slight degree of incipient melting discovered following the associated two-step treatments (Fig. 7).

As a consequence of this and the fact that no incipient melting is discovered in the specimens which are pre-homogenized at 1232°C, the 1232°C/2 hrs. + 1260°C/2 hrs./AC treatment is considered the optimum. The optimum treatment results in complete coarse  $\gamma'$  and greater than 90% eutectic  $\gamma$ - $\gamma'$  solutioning as shown in Figure 5. Additionally, specimens pre-homogenized at 1232°C for 2 hours and then further solutioned at either 1266°C or 1271°C reveal the pre-homogenized alloy's incipient melting point to be approximately 1270°C (Fig. 8).

Typical carbide microstructures of the as-cast and the 1232°C/2 hrs. + 1260°C/2 hrs./AC solutioned specimens are presented in Figure 9, illustrating that the as-cast carbide is predominantly script shaped. The as-cast carbides are MC's; Ti and Ta rich in the script cores and arms with some Cr, Hf and W involvement, with the heads of such anticipated to be Ti, Hf, Ta and W rich (particularly, Hf) based on work reported in Reference 13. When subjected to high temperature solutioning,

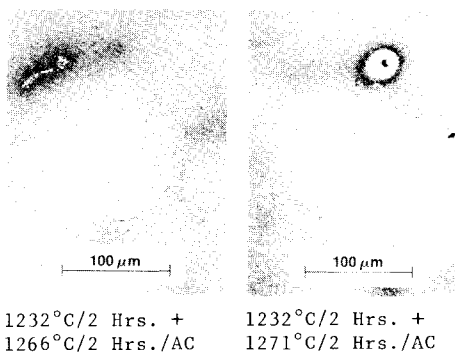


Figure 8. DS CM 247 LC two-step solutioning.

degeneration of these primary carbides occur, with relatively small/discrete secondary carbides such as  $M_{23}C_6$  and MC-3 forming. These small, discrete secondary carbides, forming at the expense of script carbide type, may be beneficial to fatigue properties as control of carbide shape and size is demonstrated to effect alloy 713C component LCF life (Ref. 14 and 15).

#### Alloy Stability

Failed rupture specimens are reviewed metallographically to determine whether the increased solutioning of the  $\gamma'$  and  $\gamma$ - $\gamma'$  eutectic constituents typical of the 1232°C/2 hr. + 1260°C/2 hr. solutioned specimens disturbed the alloy stability relative to the baseline 1221°C/2 hr. solutioned material. Like the baseline processed material, none of the failed rupture specimens (871°C/372.3 MPa/523 hrs., 982°C/151.7 MPa/554 hrs., 1093°C/68.9 MPa/329 hrs., etc.) are found to exhibit sigma, mu or alpha W formation. Slight  $M_6C$  platelet formation is observed; however, the quantity is considered insignificant and much less than typically seen in Mar M 247, where no adverse effect on the alloy's strength or ductility is apparent (Ref. 16).

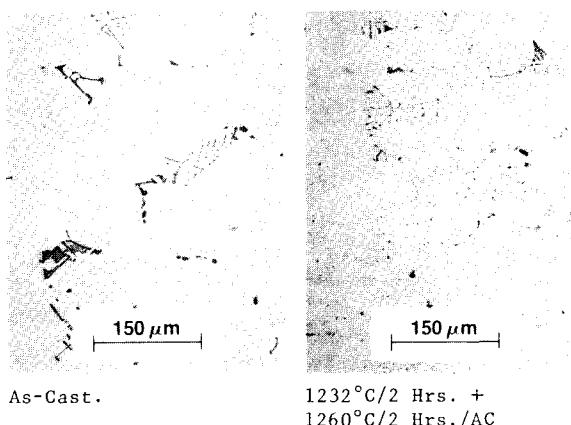


Figure 9. DS CM 247 LC typical carbide microstructure.

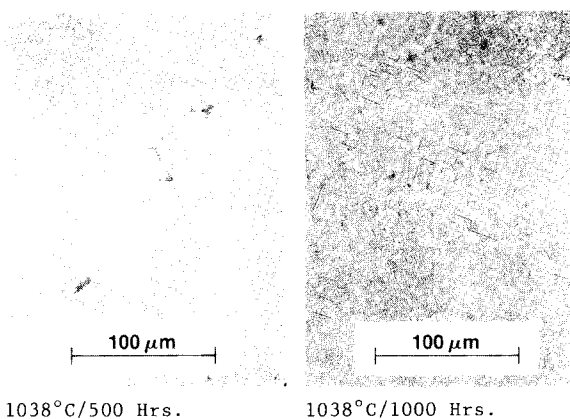


Figure 10. DS CM 247 LC  $M_6C$  formation in  $1038^\circ\text{C}$  soaked specimens.

Figure 10 illustrates the degree of  $M_6C$  formation occurring in  $1038^\circ\text{C}$ , 500 and 1000 hour soaked specimens as well as  $\gamma'$  coarsening which typically occurs under such condition. Specimens treated at  $982^\circ\text{C}$  for identical duration show no  $M_6C$  formation. Again, the amount of  $M_6C$  observed in the  $1038^\circ\text{C}$  soaked specimens is slight compared to that typical of Mar M 247 and is considered insignificant. No other instability is apparent.

#### Mechanical Properties

Both tensile and elevated temperature stress- and creep-rupture properties are enhanced by increasing test specimen volume fraction fine  $\gamma'$  through heat treatment. A nearly 10% improvement to average longitudinal RT yield and ultimate tensile strength prevails for specimens treated at the optimized, 2-step solutioned condition compared to the previously standard solution condition of  $1221^\circ\text{C}/2$  hrs/GFQ (966 MPa and 1204 MPa vs. 828 MPa and 1108 MPa). Additionally, even though strength is improved, ductility is maintained between 11-12% El. vs. 13-14% for the baseline. Note that gas fan quench (GFQ) and air cool (AC) cooling rates are similar, being approximately  $290^\circ\text{C}/\text{min}$ .

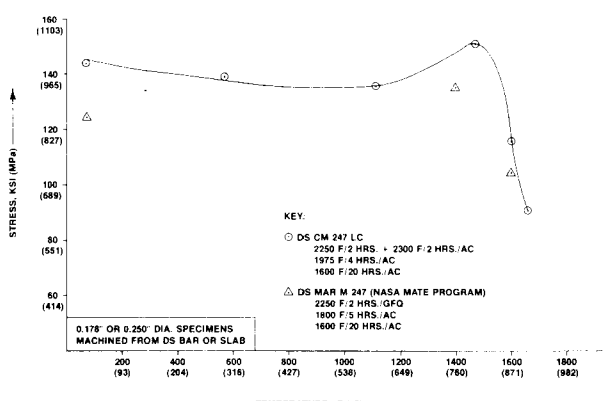


Figure 11. Average DS longitudinal 0.2% offset tensile yield strength of DS CM 247 LC vs. DS Mar M 247.

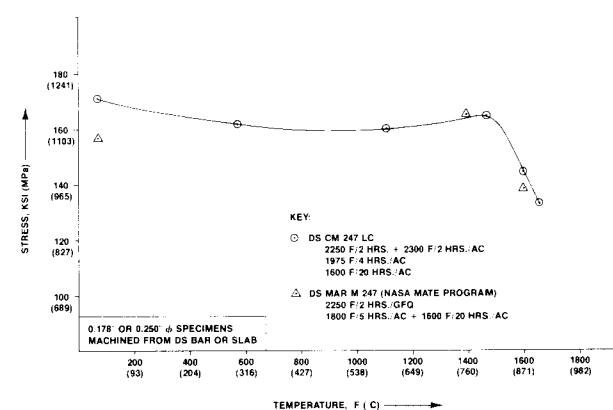


Figure 12. Average DS longitudinal ultimate tensile strength of DS CM 247 LC vs. DS Mar M 247.

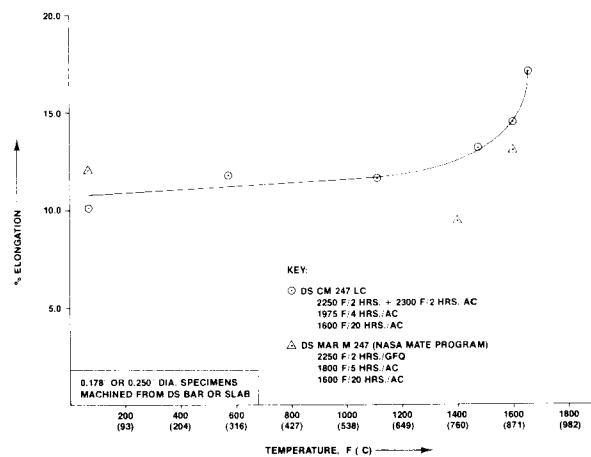


Figure 13. Average DS longitudinal tensile ductility of DS CM 247 LC vs. DS Mar M 247.

Tests utilizing various aging treatments to modify the  $\gamma'$  precipitate shape and arrangement show no effect on RT tensile properties. Figure Nos. 11 and 12 show that DS CM 247 LC exhibits better longitudinal RT- $871^\circ\text{C}$  yield and ultimate tensile strength than DS Mar M 247 solutioned at  $1232^\circ\text{C}/2$  hrs. (a condition not normally utilized in production -- normal solution for DS Mar M 247 being  $1221^\circ\text{C}/2$  hrs. which typically results in even lower tensile properties), while Figure 13 compares average ductility of the two materials.

Average DS transverse tensile test results are presented in Figure Nos. 14, 15 and 16. The DS CM 247 LC capability is compared to DS Mar M 247 between RT to  $982^\circ\text{C}$ . DS CM 247 LC exhibits higher transverse average yield and ultimate tensile strength than DS Mar M 247 throughout the test temperature range, however, shows slightly lower transverse ductility, reaching a minimum of 4.8% at  $927^\circ\text{C}$ . Note that neither DS CM 247 LC nor DS Mar M 247 exhibit transverse "nil" ductility (near 0% elongation) as reported for certain other DS superalloys transverse tensile tested in the  $760$ - $925^\circ\text{C}$  temperature range (Ref. 17).

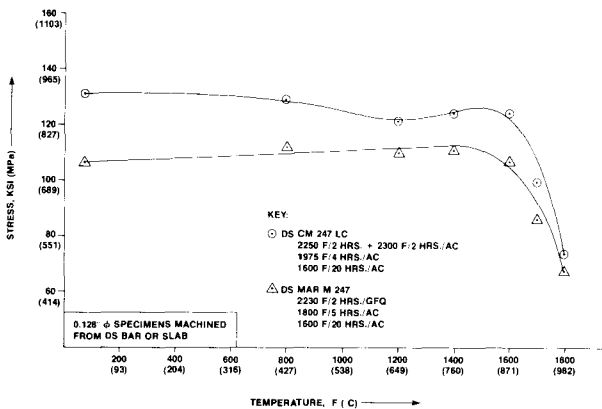


Figure 14. Average DS transverse 0.2% offset tensile yield strength of DS CM 247 LC vs. DS Mar M 247.

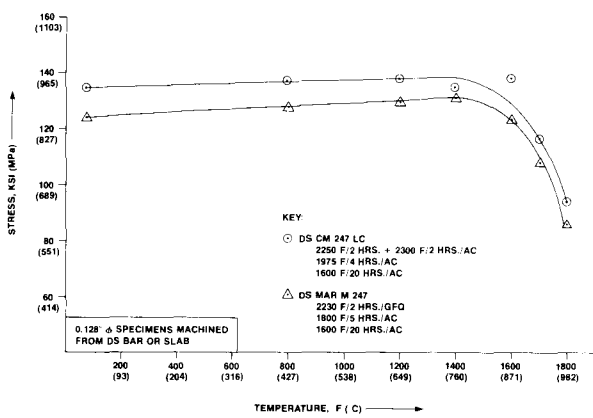


Figure 15. Average DS transverse ultimate tensile strength of DS CM 247 LC vs. DS Mar M 247.

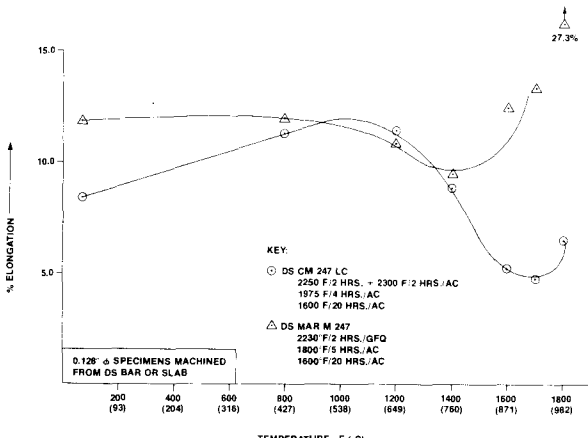


Figure 16. Average DS transverse tensile ductility of DS CM 247 LC vs. DS Mar M 247.

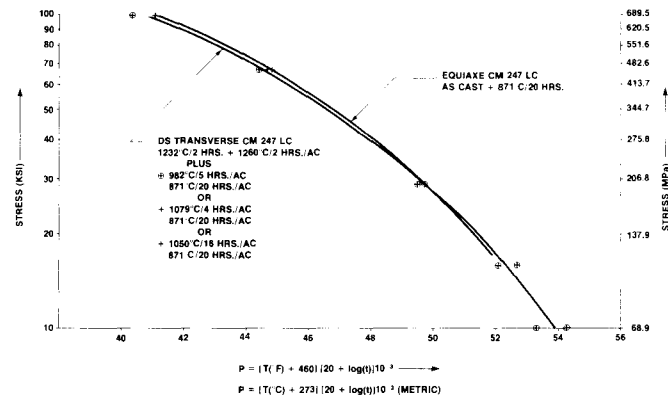


Figure 17. Stress-rupture strength of equiaxed vs. DS-transverse CM 247 LC.

DS CM 247 LC transverse Larson Miller stress-rupture properties are compared to equiaxed CM 247 LC capability in Figure 17. As anticipated, based on the satisfactory grain boundary condition (discontinuous  $M_{23}C_6$  precipitation and no  $\gamma'$  denudation--Fig. 5) observed of the specimens treated at  $1232^{\circ}\text{C} + 1260^{\circ}\text{C}$  (2 hrs. each), the alloy's DS transverse rupture properties are similar to its equiaxed counterpart.

Figure 18 illustrates the DS CM 247 LC Larson Miller longitudinal stress-rupture capability as a function of heat treatment. Clearly, the increase to test specimen volume fraction of fine  $\gamma'$  effected with two-step solutioning results in much improved metal temperature capability -- this effect occurring while also maintaining adequate ductility at 13-33% El. (4D), dependent on test condition. The increased  $V_f$  of fine  $\gamma'$  is not the only mechanism operative, but a significant contributor. Relative to the baseline  $1221^{\circ}\text{C}/2\text{ Hr.}/\text{AC}$  heat treatment, the optimized, two-step solutioning essentially effects an approximately  $23^{\circ}\text{C}$  ( $42^{\circ}\text{F}$ ) increase in rupture temperature capability throughout the entire  $345\text{--}207$  MPa,  $871^{\circ}\text{C}\text{--}982^{\circ}\text{C}$  ( $50\text{--}30$  ksi,  $1600^{\circ}\text{F}\text{--}1800^{\circ}\text{F}$ ) operating regime -- the turbine blade/vane component stress/temperature level typically experienced in advanced technology gas turbine engines.

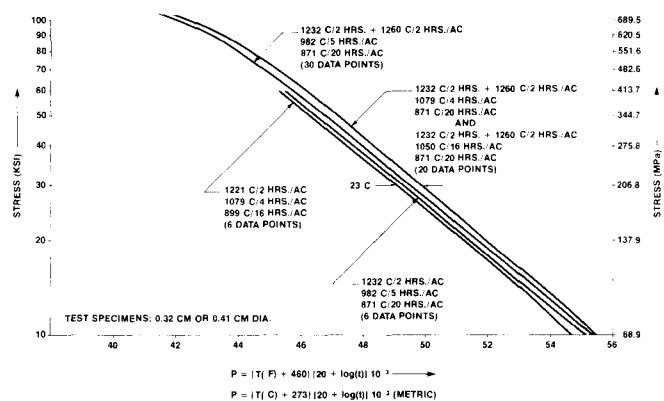


Figure 18. Longitudinal stress-rupture strength of DS CM 247 LC as a function of heat treatment.

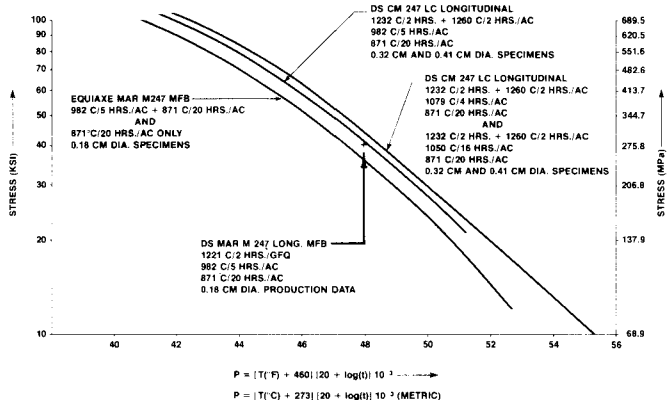


Figure 19. Stress-rupture strength of DS CM 247 LC vs. DS and equiaxed Mar M 247.

It is interesting to note that the pseudo-coating treatment chosen also affects rupture life dramatically. Direct comparison is shown in Figure 18 for specimens solutionized identically at 1232°C/2 hrs. + 1260°C/2 hrs./AC, however, pseudo-coated at either 982°C/5 hrs., 1079°C/4 hrs. or 1050°C/16 hrs. condition. The stress-rupture results attained with the 1079°C and 1050°C pseudo-coated specimens are similar, both showing significantly better creep-and stress-rupture capability than those given the 982°C/5 hr. treatment. Such variation in rupture capability is felt to be related to having aged the  $\gamma'$  at the 1079°C and 1050°C temperatures, thereby resulting in more optimum  $\gamma'$  morphology and arrangement for creep resistance. Since the 1079°C/4 hr. pseudo-coat condition represents the more realistic aluminide coating cycle, it is utilized in most property characterization.

As with RT and elevated temperature tensile properties, DS CM 247 LC (2-step solutioned) exhibits superior average longitudinal stress-rupture strength relative to both equiaxed and DS Mar M 247 (Fig. 19). Although not shown graphically, DS CM 247 LC also provides a 20°C (36°F) improvement to rupture temperature capability at the 220.6 MPa (32 ksi) stress level compared to DS MM 002 (treated at 871°C/20 hrs., only). This advantage is partially related to the DS CM 247 LC ability to be extensively solutioned, whereas MM 002 does not exhibit similar treatment capability. Note, however, that the superior strength demonstrated by CM 247 LC relative to MM 002 is also related to alloy chemical composition.

Figure 20 illustrates the stress-rupture advantage of DS relative to equiaxed CM 247 LC. This advantage, however, may be limited as the  $\gamma'$  solution tendencies are also apparent with equiaxed CM 247 LC. Such is shown in Figure 21, where a typical pseudo-coated + aged CM 247 LC equiaxed vane airfoil section microstructure is compared to a similar section which is 1232°C/2 hr. + 1260°C/2 hr./AC solutioned. Complete  $\gamma'$  and eutectic  $\gamma$  -  $\gamma'$  solutioning (without incipient melting), by two-step solutioning, will probably enhance properties; though, the potential problem continues, of course, with the grain boundary strength limitation.

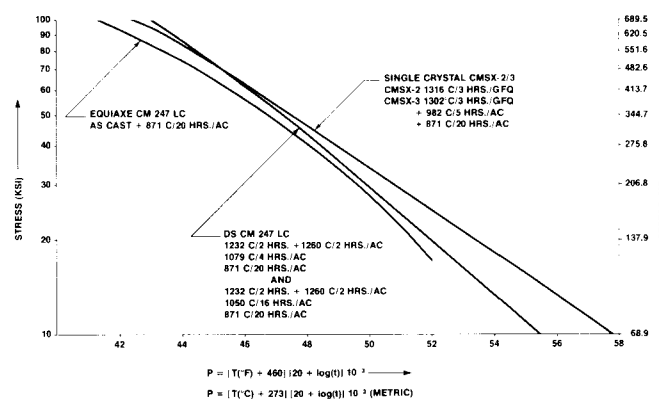


Figure 20. Stress-rupture strength of equiaxed and DS CM 247 LC vs. single crystal CMSX-2/3.

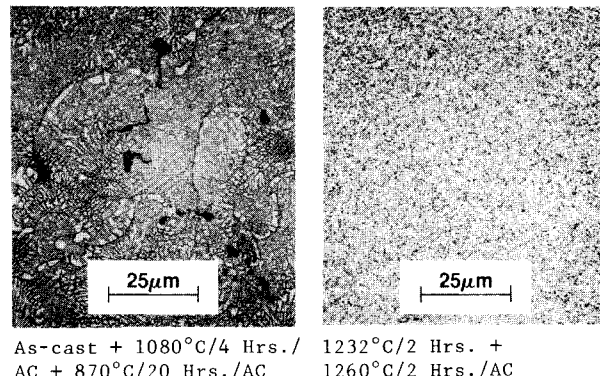


Figure 21. CM 247 LC equiaxed vane airfoil micrographs illustrating complete  $\gamma'$  and eutectic  $\gamma - \gamma'$  solutioning.

Figure 20 also shows that DS CM 247 LC approaches single crystal alloy stress-rupture capability at temperature/stress condition applicable to advanced technology gas turbine engine design. For point of reference, it is compared to the Cannon-Muskegon CMSX-2/3 alloys which exhibit similar stress-rupture strength relative to other current production single crystal alloys. Due to the DS CM 247 LC strength capability, it's likely the alloy could find application with blade or vane segments which are not easily produced in single crystal form due to problems of recrystallization which cannot otherwise be controlled, e.g., design changes or core modification. Clearly, in those instances where undersolutioning of the single crystal component is the only production option and stress-rupture properties drop to or below the DS CM 247 LC capability, DS component application would be preferred due to casting economics.

Figure 22 shows the results of HCF tests undertaken with DS CM 247 LC material solutioned according to the aforementioned optimized procedure. The results are similar to the Mar M 247 alloy capability (Ref. 18).

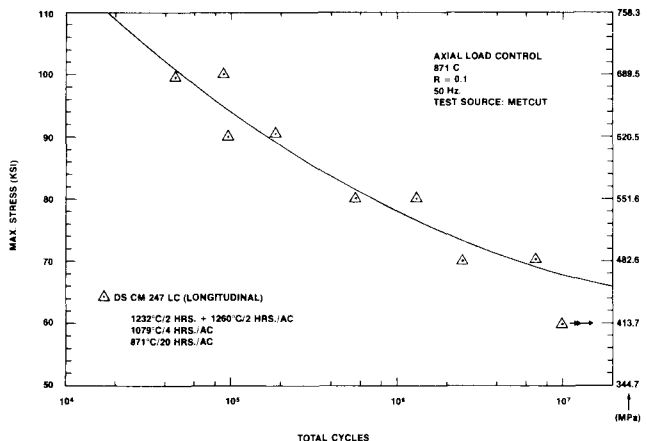


Figure 22. DS CM 247 LC, 871°C sheet specimen high cycle fatigue.

Finally, it must be noted that besides providing increased tensile and stress-rupture life, the extensive solutioning achieved with DS CM 247 LC in this investigation also improves creep rate. Table IV details selected test conditions with respective time to 1% and 2% creep for the variably treated specimens, illustrating substantial creep rate reduction.

Table IV.  
DS CM 247 LC LONGITUDINAL CREEP-RUPTURE

| Test Condition   | Heat Treatment | El. % (4D)          | RA %               | Creep 1% % | Creep 2% % | Rupture Time Hrs. |  |  |  |
|--|----------------|---------------------|--------------------|------------|------------|-------------------|--|--|--|
| 871°C/413.7 MPa<br>(1600°F/ 60.0 ksi)                                      | 1              | NA                  | NA                 | 17.5       | 31.0       | 98.4              |  |  |  |
|  | 2              | 46.0                | 48.5               | 20.5       | 35.5       | 105.9             |  |  |  |
|  | 3              | 26.5                | 40.0               | 22.0       | 116.0      | 277.1             |  |  |  |
|  | 4              | 25.1                | 39.2               | 41.0       | 93.5       | 270.8             |  |  |  |
| 871°C/372.3 MPa<br>(1600°F/ 54.0 ksi)                                      | 1              | NA                  | NA                 | 17.2       | 45.0       | 192.9             |  |  |  |
|  | 2              | 42.5                | 45.9               | 49.5       | 82.0       | 233.6             |  |  |  |
|  | 3              | 23.4                | 37.6               | 161.5      | 231.0      | 503.8             |  |  |  |
|  | 4              | 32.8                | 36.3               | 110.0      | 213.0      | 523.4             |  |  |  |
| 982°C/248.2 MPa<br>(1800°F/ 36.0 ksi)                                      | 3              | 28.9                | 55.2               | 7.5        | 16.0       | 42.0              |  |  |  |
|  | 4              | 29.7                | 50.5               | 8.5        | 17.0       | 44.6              |  |  |  |
| 982°C/220.6 MPa<br>(1800°F/ 32.0 ksi)                                      | 3              | 30.7                | 55.2               | 12.0       | 31.0       | 84.7              |  |  |  |
|  | 4              | 27.0                | 48.7               | 24.5       | 39.5       | 84.8              |  |  |  |
| 982°C/179.3 MPa<br>(1800°F/ 26.0 ksi)                                      | 1              | NA                  | NA                 | 9.2        | 35.5       | 107.3             |  |  |  |
|  | 2              | 38.7                | 53.9               | 29.5       | 62.0       | 141.3             |  |  |  |
|  | 3              | 31.8                | 60.0               | 33.0       | 96.5       | 246.7             |  |  |  |
|  | 4              | 24.3                | 46.7               | 81.0       | 129.0      | 233.6             |  |  |  |
| 982°C/151.7 MPa<br>(1800°F/ 22.0 ksi)                                      | 1              | NA                  | NA                 | 103.0      | 165.2      | 309.9             |  |  |  |
|  | 2              | 35.4                | 54.8               | 98.0       | 188.3      | 361.9             |  |  |  |
|  | 3              | 32.2                | 57.6               | 229.0      | 345.0      | 553.7             |  |  |  |
|  | 4              | 30.1                | 53.3               | 136.5      | 279.0      | 494.9             |  |  |  |
| 1038°C/144.8 MPa<br>(1900°F/ 21.0 ksi)                                     | 3              | 23.8                | 55.6               | 26.5       | 47.0       | 83.2              |  |  |  |
|  | 4              | 28.9                | 53.2               | 25.0       | 44.0       | 76.0              |  |  |  |
| Heat Treatment:  |                |                     |                    |            |            |                   |  |  |  |
| 1) 1221°C/2 hrs./AC  |                | 2) 1232°C/2 hrs./AC | 3) 1232°C/2 hrs. + |            |            |                   |  |  |  |
| 1079°C/4 hrs./AC   |                | 982°C/5 hrs./AC     | 1260°C/2 hrs./AC   |            |            |                   |  |  |  |
| 897°C/16 hrs./AC   |                | 871°C/20 hrs./AC    | 1079°C/4 hrs./AC   |            |            |                   |  |  |  |
| 4) 1232°C/2 hrs. + 1260°C/2 hrs./AC + 1050°C/16 hrs./AC + 871°C/20 hrs./AC |                |                     |                    |            |            |                   |  |  |  |
| NA - Not Available   |                |                     |                    |            |            |                   |  |  |  |

## CONCLUSIONS

- A two-step solution cycle resulting in complete coarse  $\gamma'$  and greater than 90% eutectic  $\gamma - \gamma'$  solutioning without incipient melting is established. 1232°C/2 hrs. + 1260°C/2 hrs./AC.
- Alloy tensile, stress- and creep-rupture properties are enhanced, primarily due to the increased volume fraction of fine  $\gamma'$  achieved. Alloy ductility is maintained.

The optimized solutioning procedure is the major factor increasing the alloy's stress-rupture temperature capability by 23°C (42°F) throughout the entire 207-345 MPa (30-50 ksi) stress regime, relative to the 1221°C/2 hr. "baseline" solutioned DS CM 247 LC.

- No significant instability is observed for the two-step solutioned specimens (only minor  $M_6C$  formation).
- Pre-homogenization of the cast, segregated structure is necessary to avoid incipient melting and actually raises the alloy's incipient melting temperature.
- Aging treatments designed to alter the shape and distribution of the  $\gamma'$ , enhance the 871°C tensile and elevated temperature stress-rupture capability. No effect on the RT tensile strength is observed.
- Equiaxe CM 247 LC appears to be amenable to high temperature solutioning without incipient melting. Stress-rupture property benefit may or may not occur with grain boundary strength being an important factor.

## FUTURE ACTIVITY

- Further aging treatment studies -- full  $\gamma'$  characterization.
- Define DS casting process thermal gradient effects upon component solutioning capability.
- Appropriate LCF property determinations.
- $\gamma - \gamma'$  mismatch definition.
- Grain boundary aspect ratio investigations.

## REFERENCES

- R.F. Decker (Inco Limited), "Superalloys - Does Life Renew at 50?", 4th Int'l. Symposium on Superalloys, Seven Springs, PA, Sept. 1980, p. 2.
- F.L. VerSnyder (PWA), "Superalloy Technology - Today and Tomorrow", High Temperature Alloys for Gas Turbines 1982, Liege, Belgium, Oct. 1982, p. 9.
- C. Lund (Martin Marietta), J.F. Radavich (Purdue Univ.), "Effects of Refractory Additions on the Structure and Mechanical Properties of a Hf Containing Nickel Base Superalloy", 4th Int'l. Symposium on Superalloys, Seven Springs, PA, Sept. 1980, pps. 85-98.
- K. Harris and R.E. Schwer (Cannon-Muskegon Corp.), "Vacuum Induction Refined MM0011 (Mar M 247) for Investment Cast Turbine Components", AVS 6th Int'l. Vacuum Metallurgical Conf., San Diego, CA, Apr. 1979, pps. 7-8.
- K. Harris, G.L. Erickson, R.E. Schwer (Cannon-Muskegon Corp.), "Development of a High Creep Strength, High Ductility, Cast Superalloy for Integral Turbine Wheels - CM Mar M 247 LC", 1982 AIME Annual Meeting, Dallas, TX, Feb. 1982.

6. G.L. Erickson (Cannon-Muskegon Corp.), "Cannon-Muskegon Product Evaluation Report No. 004", CM Internal R&D Report, June 1983.
7. K. Harris, G.L. Erickson, R.E. Schwer (Cannon-Muskegon Corp.), "Mar M 247 Derivations - CM 247 LC DS Alloy, CMSX Single Crystal Alloys - Properties and Performance", 5th Int'l. Symposium on Superalloys, Champion, PA, Oct. 1984.
8. G.J. DeBoer (General Electric Co.), "René 150 Directionally Solidified Superalloy Turbine Blades", NASA-MATE Project 2 Completion Report No. CR-167992, Vol. 1, Dec. 1981, p. 17.
9. G.L. Erickson, K. Harris, R.E. Schwer (Cannon-Muskegon Corp.), "Optimized Superalloy Manufacturing Process for Critical Investment Cast Components", 1984 AIME Annual Meeting, Los Angeles, CA, Feb. 1984, pps. 4-6.
10. C.L. White and D.F. Stein (Mich. Tech. Univ.), "Sulfur Segregation to Grain Boundaries in Ni<sub>3</sub>Al and Ni<sub>3</sub>(Al, Ti) Alloys", Met. Transactions, Vol. 94, Jan., 1978, pps. 13-22.
11. J.J. Jackson, M.J. Donachie, R.J. Henricks, M. Gell (PWA), "The Effects of Volume % of Fine γ' on Creep in DS Mar M 200 Hf", Met. Transactions, Vol. 8A, No. 10, 1977, p. 1615.
12. L.W. Sink, G.S. Hoppin III, M. Fujii (AiResearch), "Low-Cost Directionally-Solidified Turbine Blades, Volume 1", NASA Report No. CR-159464, Jan. 1979.
13. S.W. Wawro (Purdue Univ. Student), "MC Carbide Structures in Mar M 247", NASA Contractor Report No. 167892, June 1982, p. 24.
14. Ibid 9, pps. 8-9.
15. M. Lamberigts (CRM), G. Ballarati, J.M. Drapier (FN-Formetal), "Optimization of the High Temperature, Low Cycle Fatigue Strength of Precision-Cast Turbine Wheels", 5th Int'l. Symposium on Superalloys, Champion, PA, Oct. 1984.
16. Ibid 12, p. 152.
17. S.W. Yang (G.E.), "Tensile Ductility of Monocrystalline Superalloys", 1984 TMS-AIME Fall Meeting, Detroit, MI., Sept. 19, 1984.
18. R.J. Wagner (Garrett Turbine), Verbal Communication, Dec. 1984.